

## Water/Alcohol Mixtures: A Spectroscopic Study of the Water-Saturated 1-Octanol Solution

Paola Sassi,<sup>\*,†</sup> Marco Paolantoni,<sup>†</sup> Rosario Sergio Cataliotti,<sup>†,‡</sup> Francesca Palombo,<sup>†</sup> and Assunta Morresi<sup>†</sup>*Dipartimento di Chimica, Sezione di Chimica Fisica, Università di Perugia, Via Elce di Sotto 8, I-06123 Perugia, Italy, and Istituto Nazionale di Fisica della Materia, Unità di Catania, 95100 Catania, Italy**Received: July 28, 2004*

The properties of the water-saturated 1-octanol solution in the 10–75 °C temperature range have been investigated by means of different scattering spectroscopies. The results of Raman, depolarized-Rayleigh, and Rayleigh–Brillouin experiments have been compared to the corresponding results recently obtained for the pure alcohol in our laboratory. Spectroscopic findings obtained for the temperature behavior of vibrational, rotational, and translational degrees of freedom are analyzed according to a single, unifying picture of this liquid system. Differences and analogies between pure and water-saturated 1-octanol suggest the key for interpreting the structural properties connected to the amphiphilic nature of *n*-alcohols. In a wider perspective, the same arguments can be applied to the study of larger and more complicated systems such as phospholipids for which 1-octanol represents a simple model.

## 1. Introduction

The properties of water dissolved in amphiphilic molecular liquid systems have been widely explored in the case of low molecular weight normal alcohols (*n*-OH). This is a situation in which the two components of the solution are completely miscible; nevertheless, the alcohol–water solutions show negative mixing entropy.<sup>1,2</sup> These experimental evidences, especially in the case of water-rich solutions, have been referred to as examples of acting hydrophobic interactions.<sup>3–5</sup> Recent Raman and neutron scattering experiments,<sup>6,7</sup> and dielectric relaxation measurements,<sup>8</sup> attribute the phenomenon to incomplete mixing at the molecular level rather than to water restructuring from hydrophobic moieties.

Still referring to *n*-OH, when the hydrophobic part of the molecule becomes increasingly long ( $C_n$ ,  $n > 4$ ), the water–alcohol interactions cannot be followed through the entire composition range ( $0 < x < 1$ ). In butyl alcohols, the water solubility is also reduced on going from normal- to iso- and then to *sec*-butanol: the only exception is given by *tert*-butyl alcohol that is soluble in all proportions.<sup>9</sup> Because of its almost spherical molecular shape, its accommodation into the water structure is made easier, even with the peculiarities shown by  $(CH_3)_3COH$  in the different regions of the composition range.<sup>10–12</sup>

In long-chain liquid *n*-OH, the affinity of the hydroxylic functionality toward water is not sufficient to allow a favorable solubilization. Because of the strong cooperativity in the H-bonding network of  $H_2O$ , the extended apolar regions constituted by methylenic chains of *n*-OH hardly succeed in causing distortion of the water structure, and this fact certainly reduces the miscibility.

Actually, the accessibility of water to polar cores in liquid bulk structure of long-chain *n*-OH seems to be connected to the small dimensions of  $H_2O$  clusters rather than to the H-bonding water–alcohol interactions. The 1-octanol–water

solutions studied in our laboratory by means of stationary spectroscopic scattering techniques offer good illustration of such a behavior.

We prepared the two saturated water-rich and octanol-rich solutions by mixing the two liquids at room temperature and separating the relevant layers after the partition equilibrium was achieved. Spectroscopic measurements of the two solutions were performed after hours from preparation.

In Figure 1, the Raman spectra of pure liquids and relevant mixtures are shown. From the comparison evidenced in the figure, one can see that the Raman spectroscopy is not sensitive to reveal the scattering signal coming from the octanol contained in the water-rich solution layer (right graph of Figure 1). This is a bit surprising, knowing that the CH stretching Raman signals of 1-octanol are very intense (left graph of Figure 1). According to this finding, we believe that, for the analysis of our results, it is reasonable to assume that 1-octanol is not dissolved in water at least within the sensitivity limits of Raman technique. On the contrary, we find evidence of the water content in the octanol-rich solution (inset of left part of Figure 1).

For this reason, in the following we will present and discuss the results obtained for the octanol-rich solution, which represents the saturation limit of water in pure octanol.

The comparison with relevant data of the pure liquid evidences that the 1-octanol liquid structure is essentially unchanged after water addition. This result is absolutely not obvious because recent molecular dynamics simulations<sup>13</sup> would rather suggest an increase of octanol cluster dimensions in the proximity of water molecules. Nevertheless, the structure and dynamics of solution probed with different scattering techniques show no evidence of any modification of alcohol properties. As a consequence, a microinhomogeneity of the liquid system can be considered, and the existence of “pockets” containing high-density water can be assumed. In this respect, the properties of these water pockets offer an example of spatial confinement on a scale smaller than mesoscopic: we define this phenomenon as “molecular confinement”.

\* Corresponding author. E-mail: sassipa@unipg.it.

<sup>†</sup> Università di Perugia.

<sup>‡</sup> Istituto Nazionale di Fisica della Materia.

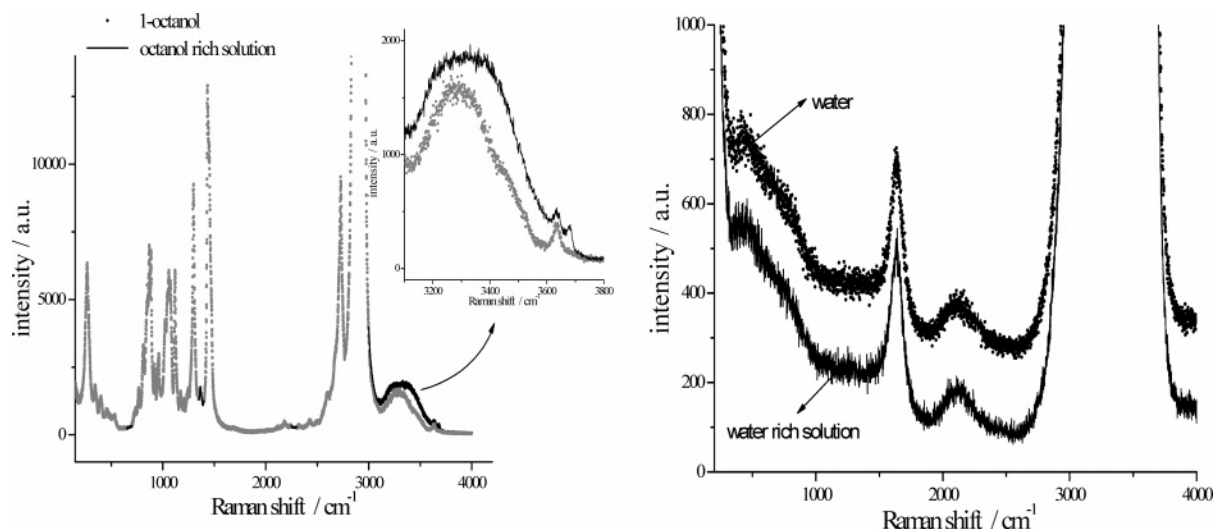


**Figure 1.** VV Raman spectra profiles of pure 1-octanol, water, and saturated solutions at 25 °C. The inset in the left part of the figure shows the differences between the OH-stretching profile of 1-octanol and octanol-rich solution.

## 2. Experimental Section

1-Octanol was purchased from Fluka with 99.5% purity and was used without any further purification treatment. Before depolarized-Rayleigh (DR) and Rayleigh–Brillouin (RB) measurements were executed, the sample was filtered directly in the appropriate measure cuvette with a Millipore filter of 0.22  $\mu\text{m}$ .

Bidistilled and deionized liquid water was prepared in our laboratory. The purity of the liquid was controlled by IR and Raman spectra, reproducing the literature features.

Next, 100 mL of the two liquids was mixed under energetic stirring, and the two layers were allowed to separate in a partition funnel. Both layers were analyzed, giving the results reported in Figure 1.

The Raman spectra of pure octanol and octanol-rich solution were collected both in VV and in HV polarization geometry, exciting the samples with the 514.5 nm radiation of a COHERENT argon ion laser, model Innova 90, and focusing a power of 700 mW on the cuvette. The dispersive tool was an ISA-Jobin-Yvon U-1000 double monochromator, having holographic gratings with 1800 lines/mm and a focal length of 1 m. The signals were revealed with an electronically cooled Hamamatsu photomultiplier model R943 and, through a photon counting chain, were sent to an on-line PC that was used for acquisition and elaboration of rough experimental data. The polarization measurements of the scattered radiation were recorded with Melles-Griot optics, previously standardized over the 459  $\text{cm}^{-1}$  band of  $\text{CCl}_4$ .

DR and RB spectra were acquired by irradiating the sample with the monomode (Etalon intracavity) 514.5 nm radiation of a COHERENT argon ion laser with a power of 300 mW over the sample. By placing the free spectral range of our single pass piezoscanned Fabry–Perot interferometer (Burleigh RC-110) at the value of 20 GHz, with a finesse of ca. 30, we can record 3 orders of the interferometric trace. The statistics of measurement were improved further with many (at least 10) acquisitions. The width of the instrumental function and alignment conditions of the interferometric apparatus were detected by measuring the scattered signals coming from a static scatterer, for example, latex suspended nanoparticles. After deconvolution of the instrumental function, the evaluation of Rayleigh bandwidth and Brillouin bandwidth and position was accomplished with a curve-fitting procedure performed simultaneously on the three

**TABLE 1: Physicochemical Properties of Saturated Octanol Solution at 25 °C**

$V_{\text{water}}^{19}$ $\text{cm}^3 \text{mol}^{-1}$	$V_{\text{octanol}}$ $\text{cm}^3 \text{mol}^{-1}$	$\rho_M$ $\text{g cm}^{-3}$	$x_{\text{water}}$
17.92	158.92	0.825	0.26

interferometric orders. This allowed us to take into account the possible superposition of adjacent Stokes–anti-Stokes components.

All measurements were performed in the 10–70 °C temperature range using a Haake model F6 ultrathermostat, with circulating water and temperature control accuracy of  $\pm 0.5$  °C.

## 3. Results and Discussion

In previous papers,<sup>14–18</sup> we performed a detailed analysis of dynamical and structural properties of pure octanol using different spectroscopic techniques; we have adopted the same strategy to perform the study of the water-saturated solution (hereafter named SAT).

From experimental values of mass density, we estimated the molar fraction of water in SAT ( $x_{\text{water}}$ ), referring to available values of partial molar volumes of  $\text{C}_8\text{H}_{17}\text{OH}$  and  $\text{H}_2\text{O}$  in this mixture as reported by Berti et al.<sup>19</sup> (see Table 1). These authors explicitly say that the 1-octanol molar volume in solution is essentially the same as that of the pure alcohol and that, on the contrary, the water molar volume is lower with respect to the pure liquid. The  $x_{\text{water}} = 0.26$  value calculated from our density measurements at 25 °C and reported in Table 1 is in perfect agreement with existing experimental<sup>20</sup> and computational<sup>13,21</sup> data.

**3.1. Comparison between Pure Alcohol and Solution.** We start by comparing Raman spectra of pure 1-octanol and octanol-rich solution to follow possible modifications of the alcohol liquid structure caused by the presence of water.

As the left part of Figure 1 shows, there is no modification of the 1-octanol Raman spectrum except for the high-frequency region, when water is dissolved at the saturation limit. In Figure 2, the temperature evolution of the OH-stretching mode of SAT, both VV and HV configurations, is shown.

The comparison of pure and water-saturated alcohol suggests that, except for the interactions regarding the hydroxylic oscillator, the properties of the 1-octanol bulk liquid structure do not show significant changes in the whole temperature range.

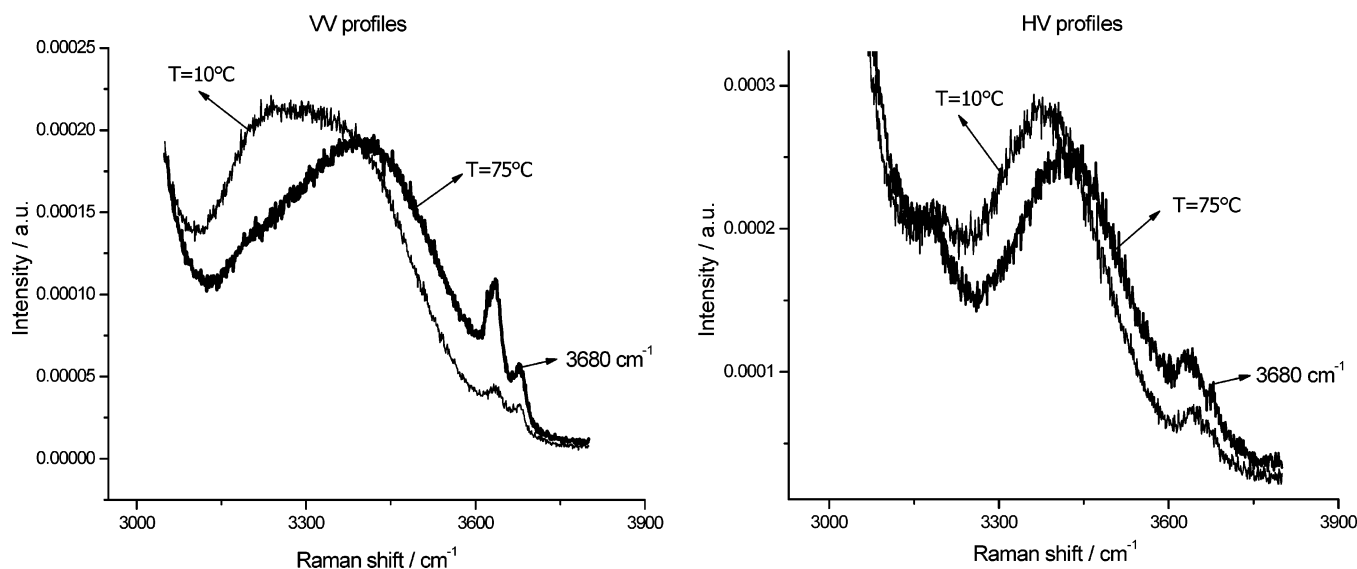


**Figure 2.** Octanol-rich solution: Raman VV and HV spectra in the OH-stretching region at extreme working temperatures.

Similar results have also been found in methanol-rich water solution.<sup>6</sup> In this case, the authors propose a hydration regime in the  $1 > x_{\text{alcohol}} > 0.7$  composition range where water molecules are H-bonded to terminal OH groups of alcohol aggregates. Sato et al. derived reorientational relaxation data for the propanol/water mixture using dielectric spectroscopy,<sup>8,22,23</sup> proposing the same chain-end hydration mechanism of the alcohol-rich solutions. According to these interpretations, the structure of liquid alcohol is not perturbed by the addition of water until the content of H<sub>2</sub>O is such to break the alcohol aggregates, thus solvating the molecules individually. The question now arises: is the water content corresponding to the saturation limit of SAT really enough to perturb the consistent hydrophobic and hydrophilic interactions present in 1-octanol, or does it leave the alcohol structure almost unchanged? We will try to answer this question with the following discussions.

Our results concerning the Raman spectrum of neat liquid and SAT indicate the absence of detectable perturbations localized in the vibrations of the hydrocarbon chain. On the contrary, in short-chain *n*-OH, the C–H stretching vibration is sensitive to the presence of water. In particular, a monotone increase of the frequency of this signal detectable even for very low water concentrations has been found.<sup>6,10–12</sup> This situation has generically been connected with environmental changes felt by the alkylic portion of alcohol molecules and induced by water.

A computer simulation study performed on neat and hydrated 1-octanol<sup>13</sup> suggests that the addition of water should cause a restructuring of the H-bonding network of liquid octanol, thus increasing the average number of molecules per aggregate and identifying regions with strong polar character. This restructuring of H-bonding interactions suggested by MacCallum and Tieleman could be in accord with our Raman data concerning the high-frequency region. In fact, it should change in some way the intensity distribution of oscillators contributing to the OH-stretching band shape, as it seems to occur in our Raman spectra.

On the contrary, our Brillouin (RB) and depolarized-Rayleigh (DR) scattering data do not evidence any significant perturbation of structural and dynamical properties of the liquid alcohol.

**3.2. Dynamics and Structure Probed in the GHz Frequency Range.** DR and RB experiments are particularly insightful in revealing the collective properties of liquids and therefore long-range correlations.

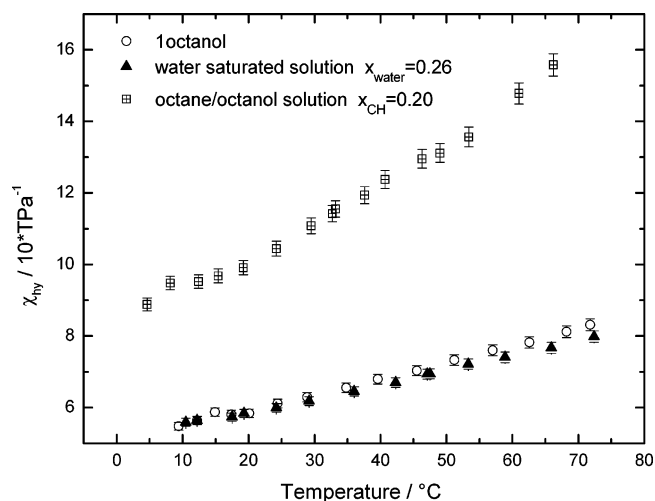


**Figure 3.** Compressibility data of 1-octanol ( $x_{\text{water}} = 0.26$ ), and octane/octanol ( $x_{\text{CH}} = 0.20$ ) solutions obtained by Rayleigh–Brillouin measurements.

RB spectroscopy probes the propagation and damping of the longitudinal acoustic modes; the values of hypersonic compressibility obtained from the Brillouin line shift give a measure of structural “rigidity” of the involved liquid system.

Hypersonic compressibility  $\chi_{\text{hy}}$  values have been recently reported for 1-octanol/octane solutions.<sup>17</sup> In this study, we demonstrated that the hypersonic compressibility, as detected by Brillouin experiment, is very sensitive to temperature and dilution effects, being a powerful probe of both self-association and solute/solvent volume accommodation properties in solution. We showed how these two “H-structure” and “volume” effects contribute in determining the structural properties of 1-octanol/octane solutions. Moreover, we observed that octane addition causes large variation of the system compressibility. In Figure 3, together with the data of SAT and pure octanol, we plot the  $\chi_{\text{hy}}$  values obtained for a solution of  $x_{\text{CH}} = 0.20$  octane in octanol, with  $x_{\text{CH}}$  as the alkane molar fraction. Thus, although we are comparing aqueous and alkane solutions having a similar concentration of octanol, the compressibility data show that the effect produced by the addition of octane is much more pronounced than that of water. Moreover, even the temperature effects on  $\chi_{\text{hy}}$  values are much more evident in octane than water solution.



In the case of modification of the H-bonding network because of the presence of water, we could expect a sensitive variation of compressibility at different temperatures. We know from density measurement that the liquid  $\text{H}_2\text{O}$  in SAT has a density higher than that of pure water;<sup>19</sup> as a consequence, the contribution of this component to the  $\chi_{\text{hy}}$  value of the mixture should enhance the rigidity of the system. On the contrary, the data reported in Figure 3 show that the addition of water to octanol does not sensitively change the compressibility of the liquid: the comparison between pure liquid and SAT shows that the differences tend to appear only around 60 °C and above. With this respect, we do not believe that it depends on a scarce sensitivity of the Brillouin technique because the octanol/octane solution markedly highlights the differences with the pure liquid. It could rather depend on the fact that the properties of the water/octanol system at this concentration are dominated by those of liquid alcohol and that this component of the mixture may not be characterized by a completely different H-bonding network, nor by a different arrangement of alkylic tails. Even if we assume that the octanol self-aggregation is not perturbed, the slight decrease observed for  $\chi_{\text{hy}}$  values of SAT with respect to pure octanol could be justified by assuming that the only effect of water addition is to fill the free volume of liquid alcohol without any perturbation of its molecular and supramolecular structure.

This assertion is in agreement with findings of Sato et al.<sup>22,23</sup> on short-chain *n*-OH. In aqueous methanol, ethanol, and propanol, the excess activation enthalpy and entropy of the main dielectric relaxation process are close to zero, suggesting that in alcohol-rich solutions the components of the mixture are in almost the same environment as the pure liquids.

DR experiments in the GHz frequency range offer the possibility of estimating relaxation times directly related to reorientational molecular motion. For liquid 1-octanol, such a dynamics corresponds to a relaxation time  $\tau^{\text{DR}}$  of hundreds of picoseconds<sup>14</sup> and refers to a relaxation process involving reorientation of hydrogen-bonded aggregates and aggregates "turnover".<sup>21</sup> The detected dynamics is due to the relaxation of the total anisotropic polarizability of the system and may result from complex collective motions not easily explicable at the molecular level. At the moment, it is also not clear to what extent the slow DR relaxation time can be related to the long time relaxation detected by dielectric experiments.<sup>21–24</sup> In any case, DR spectral profiles, depending on long-range intermolecular interactions and on the extent of hydrogen bonding, are potentially sensitive to overall restructuring changes that eventually occur in the liquid system. This situation has been evidenced in a previous DR study performed in pure liquid 1-octanol at different temperatures.<sup>14</sup>

Figure 4 shows that DR relaxation times of neat 1-octanol and SAT are practically coincident within experimental uncertainties. Because DR experiments could sensitively probe restructuring changes induced by the presence of water, the results of Figure 4 indicate that water addition leads to minor changes in the long-range structure of the neat 1-octanol.

In contrast to the behavior depicted in Figure 4, it has been shown that the slow dielectric relaxation time is largely dependent on water content, showing a value that decreases on increasing water fraction for both short- and long-chain normal alcohols.<sup>25–27</sup> This fact suggests that the two relaxation mechanisms obtained by DR and dielectric techniques do not have a common origin. Interestingly, the value of  $\tau^{\text{DR}}$  in pure 1-octanol and SAT is very close to the ultrasonic relaxation time reported

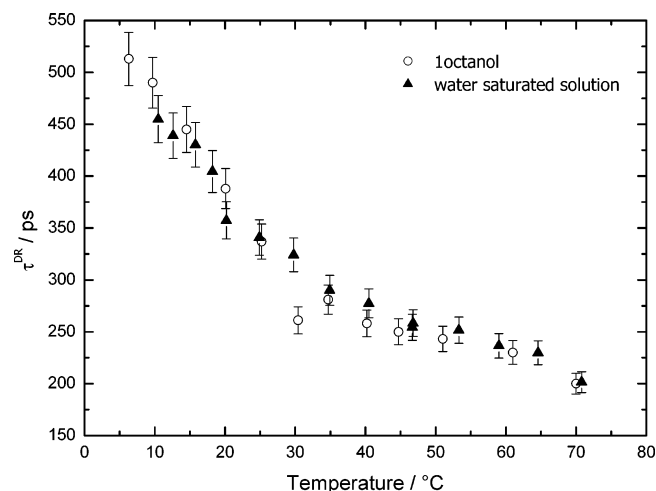


**Figure 4.** Relaxation times obtained from interferometric depolarized-Rayleigh measurements.

by Behrends and Kaatz,<sup>28</sup> so that some correlation between the two processes can be envisaged.

Considering that light-scattering experiments are more directly connected with dynamical properties of hydrophobic moieties rather than with those of polar heads, it is not surprising that the relaxation phenomenon probed by DR does not depend on the presence of water molecules mainly localized in the proximity of hydrophilic regions. This is expected as long as the presence of water does not produce substantial modifications of the intrachain *n*-OH liquid structure.

**3.3. Water–Alcohol Interactions.** We believe that a reasonable interpretation of all of our data regarding the behavior of vibrational, rotational, and translational degrees of freedom of SAT can be given if we assume that the liquid structure of 1-octanol remains essentially the same in pure liquid and in the water-saturated solution. Thus, the differences in the OH-stretching region of the Raman spectrum are essentially due to the scattering intensity of the water fraction in solution. In other words, the modifications observed in this spectral range are due to a simple superimposing of OH Raman cross sections of *n*-octanol and water.

This assumption corresponds to one saying that the two components of the mixture show reduced interactions and that the solution shows microheterogeneous domains because alcohol–alcohol H-bonds are not disrupted in favor of alcohol–water interactions. As a consequence, the amount of water at the saturation limit is not homogeneously distributed in the volume of the sample because of two reasons: (a) it is highly improbable that the water molecules can occupy spaces in the proximity of alkylic chains; (b) the H-bond between alcohol (A) and water (W) molecules is not preferred with respect to A–A and W–W interactions. This does not mean that A–W H-bonding interaction is not likely to be found in solution: it rather means that this interaction does not destroy the long-range structure of liquid octanol, being at most localized around the OH terminals of alcohol clusters or free molecules. Moreover, with the relatively small quantity of water, this situation regards only restricted regions of the bulk liquid; as a consequence, we could refer to the existence of “water pockets” in solution similar to those suggested for aqueous solution of *tert*-butyl alcohol.<sup>5</sup>

One of the experimental data that support the “segregation” of water molecules in the so-called “pockets” in the hydrophilic regions is the presence in the spectrum of SAT of the high-frequency (ca. 3680  $\text{cm}^{-1}$ ) Raman band that is commonly assigned to monomeric water.<sup>30,31</sup> Despite the large disposability

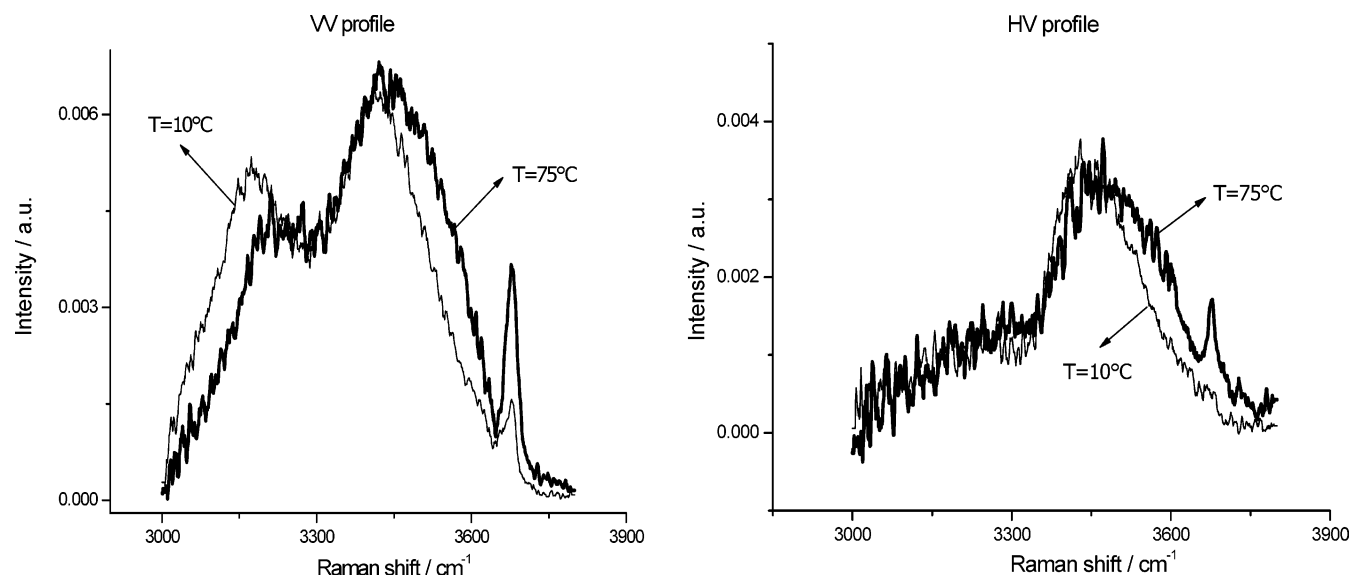


**Figure 5.** Subtraction spectra (octanol-rich solution – pure octanol): VV and HV profiles in the OH-stretching region at two different temperatures.

of OH functionality from liquid alcohol, the presence of water that is little involved in the H-bonding network of 1-octanol is clearly revealed in both VV and HV profiles at each temperature (see Figure 2).

Actually, we think that the study of the spectral properties of SAT is very important to obtain a double result. On one side, we can follow the characteristics of amphiphilic nature of normal alcohols by comparing our data with those of the water solution of shorter chain alkanols. On the other side, we can characterize the polar cores of SAT, by comparing the data of solution with that of pure water (see section 3.5).

Referring to the first of these two aspects, we think that our findings are not far from the results obtained for methanol- and propanol-water solutions,<sup>6–8</sup> even if it is not possible to associate a component of the spectrum to the chain-end hydration of alcohol aggregates. As well as for shorter chain alkanols, we do believe in the existence of microheterogeneous structure of alcohol-rich solutions, and we also agree with the assumption of the hydration mechanism leaving the arrangement of self-aggregating *n*-OH almost unchanged.

If we look at the results of Dixit et al.,<sup>6,7</sup> we see that the hydration condition reported above is realized when  $0 < x_{\text{water}} < 0.3$  in methanol solutions: at higher water content, the self-association of CH<sub>3</sub>OH molecules via H-bonding is strongly perturbed. In water-octanol solution, this latter situation is never reached and the A–W interaction never succeeds in destroying A–A self-aggregation.

Interestingly, the saturation condition in octanol ( $x_{\text{water}} = 0.26$ ) is realized at the same value of  $x_{\text{water}}$  at which the hydration condition of methanol changes. This experimental evidence of important analogies between short- and long-chain *n*-OH gives great effort to the possibility of extending the discussion to even larger amphiphiles. As a consequence, we can really give an explanation of the assumption that simple alcohols are good models for macromolecules in solution.

Considering that the strength of hydrogen bonding in *n*-OH is not sensitive to chain length,<sup>29</sup> we can understand why the addition of a little amount of water to pure alkanols produces almost the same effect on methanol and octanol structures. On the contrary, the steric hindrance of alkylic chain is largely affecting the miscibility of constituents when  $x_{\text{water}} > 0.3$ ; in this case, the hydrophobic interactions compete with the

hydrophilic interactions, and the possibility of hydrating the alkylic chain is more and more reduced on increasing chain length.

**3.4. Subtraction Spectra.** The assumption that the two components of SAT are weakly or not interacting suggests operating a subtraction of Raman spectra to isolate the contribution of water to the solution. Each spectrum of 1-octanol at a temperature  $T_i$  has been subtracted from the spectrum of solution at the same temperature; the same procedure has been applied to both VV and HV profiles. To achieve a better subtraction, all Raman spectra have been normalized to the integrated intensity of CH stretching bands, and then subtracted in the 3000–3800 cm<sup>−1</sup> region. The normalization condition on CH stretching intensity was adopted after verifying that this signal intensity is composition independent. The results are shown in Figure 5: in this figure, only the subtraction spectra at the extreme working temperatures are selected to give a clear image of the temperature behavior.

The result of spectral subtraction is very interesting because it suggests a series of important considerations about the properties of water in the octanol-rich solution.

First, it is possible to recognize at least three components of OH-stretching band at ca. 3680, 3400, and 3200 cm<sup>−1</sup>; it is also possible to see that the components are not strongly polarized except for the low-frequency one.

The spectroscopic study of bulk water in this spectral region usually suggests an interpretation of the structural properties of the liquid system.<sup>32–36</sup> According to this, the low-frequency component (OH<sub>1</sub> at ca. 3200 cm<sup>−1</sup>) is assigned to the collective in-phase OH-stretching mode of ordered and tetrahedrally coordinated water. It has been shown<sup>37</sup> that this component shifts to the Ice' (I<sub>h</sub>) spectrum band at ca. 3100 cm<sup>−1</sup> or to the amorphous solid spectrum at 3135 cm<sup>−1</sup>, by lowering the temperature in the supercooling region around −32 °C.

On the contrary, the high-frequency contours (OH<sub>2</sub> at 3400 cm<sup>−1</sup> and OH<sub>3</sub> at ca. 3680 cm<sup>−1</sup>) may be referred to water molecules in which the H-bonds are distorted or broken to some extent. In particular, the 3680 cm<sup>−1</sup> band is assigned to “free” OH oscillators of water molecules.

The properties of our subtraction spectra fit with the assignment of liquid water even if the general aspect is not perfectly coincident with that of the bulk liquid. To perform a check of this statement, we have measured pure water under the same

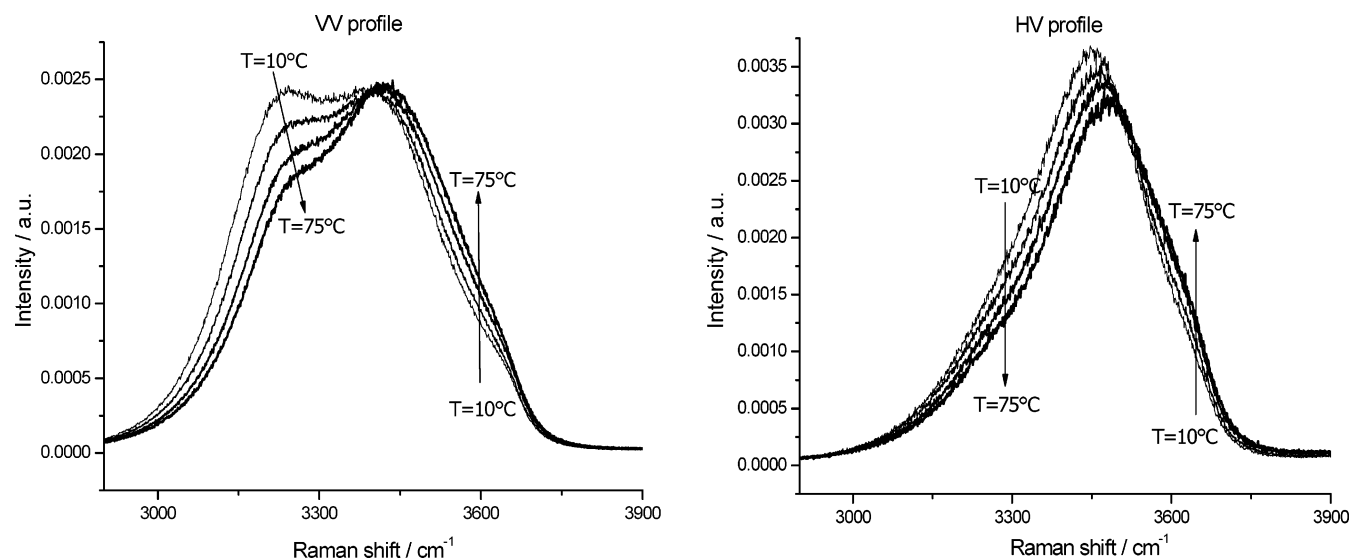


**Figure 6.** Pure liquid water: VV and HV profiles in the OH-stretching region at different temperatures.

**TABLE 2: Water in Octanol-Rich Solution: Curve-Fitting Results Obtained for the VV Subtraction Spectra**

temp/°C	OH <sub>1</sub>		OH <sub>2a</sub>		OH <sub>2b</sub>		OH <sub>3</sub>	
	center	intensity %	center	intensity %	center	intensity %	center	intensity %
10	3172	36.9	3414	43.5	3557	12.2	3675	7.3
15	3178	34.8	3415	40.4	3546	15.2	3677	9.6
25	3186	32.1	3418	42.0	3540	15.6	3676	10.3
35	3200	30.3	3418	38.6	3540	18.3	3676	12.9
45	3207	29.1	3418	39.4	3554	19.4	3676	12.1
55	3210	26.9	3421	38.9	3557	20.1	3675	14.1
65	3214	28.2	3415	31.2	3540	16.2	3677	16.2
75	3218	25.1	3414	33.1	3541	23.5	3676	18.4

experimental conditions of the solution (Figure 6). The comparison of the two samples shows that the broad features of pure liquid water are reproduced in the subtraction spectra and, even if each component is sharper in SAT, the temperature behavior is reproduced too. This is verified for the frequency shifts and the relative intensity variations observed for the bands around 3200 and 3400  $\text{cm}^{-1}$ ; they behave as do their corresponding values of pure water in the same temperature range.

Thus, despite the low signal/noise ratio, the profiles obtained with spectral subtraction allow the characterization of water in octanol solution.

**3.5. Water in Octanol at Saturation Limit.** The similarities shown in Figures 5 and 6 seem to confirm our procedure of isolating the contribution of water from the spectrum of SAT without considering consistent perturbations to the scattering of 1-octanol. As a consequence, we are confident about the possibility of revealing by means of Raman spectroscopy the structural properties of water pockets dissolved in a low polarity, amphiphilic solvent.

**3.5.1. Spectroscopic Properties.** The mixture under study is close to the above-mentioned situation of  $\text{H}_2\text{O}$  solubility in low molecular weight  $n\text{-OH}$ . Moreover, it is also similar to the situation of  $\text{H}_2\text{O}$  solubility in large biomolecules. In fact, the water–octanol binary system is largely applied as a reference standard in simulating the partition coefficients of drugs in living membranes,<sup>38–40</sup> because its amphiphility is comparable to that of phospholipidic membrane components. In light of our results, we think that this property is essentially due to the presence of extended hydrophobic regions confining water in the proximity of polar heads of alcohol molecules. This water confinement is, however, different from what is possible to observe in

hydrocarbons,<sup>31,41</sup> because the characteristics of bulk water are completely lost in alkane but partially maintained in alcohol solutions.

It is possible to see that the OH<sub>1</sub> band is present in the VV spectrum of Figure 5 also at the higher temperatures. Its polarization properties shown by comparison of polarized and depolarized profiles suggest that the spectral features found after subtraction are those of liquid water and not an artifact of manipulation: in fact, they are consistent with the assignment to the symmetric, collective icelike mode of bulk water.<sup>37</sup> As well as in pure water, the low-frequency OH<sub>1</sub> component shows a sensitive blue shift on increasing temperature especially in VV configuration spectra.

The temperature behavior of OH<sub>2</sub> is similar to that of OH<sub>1</sub> according to the frequency shift, but opposite in intensity variation. In the case of OH<sub>2</sub> component, the blue shift seems rather to be connected to the different behavior of two subbands. To this extent, we performed a curve-fitting analysis of VV subtraction profiles at the different temperatures. The refining procedure has given its best result by using four different Gaussian components, thus reproducing the total OH<sub>2</sub> profile with the OH<sub>2a</sub> and OH<sub>2b</sub> components. This procedure has not been applied to the HV profiles subtraction spectra because of the very low signal/noise ratio especially in the 3000–3300  $\text{cm}^{-1}$  region. Results of such a four-component band-fitting analysis are reported in Table 2 and are shown in Figure 7 at two temperatures.

From the data of Table 2, is possible to see that the increasing temperature produces the effect of declining intensity and shifting to the blue of the OH<sub>1</sub> band. The same trend is observed in the spectra of pure water for the component at ca. 3200  $\text{cm}^{-1}$ .<sup>37</sup> OH<sub>3</sub> almost maintains its position, but the intensity

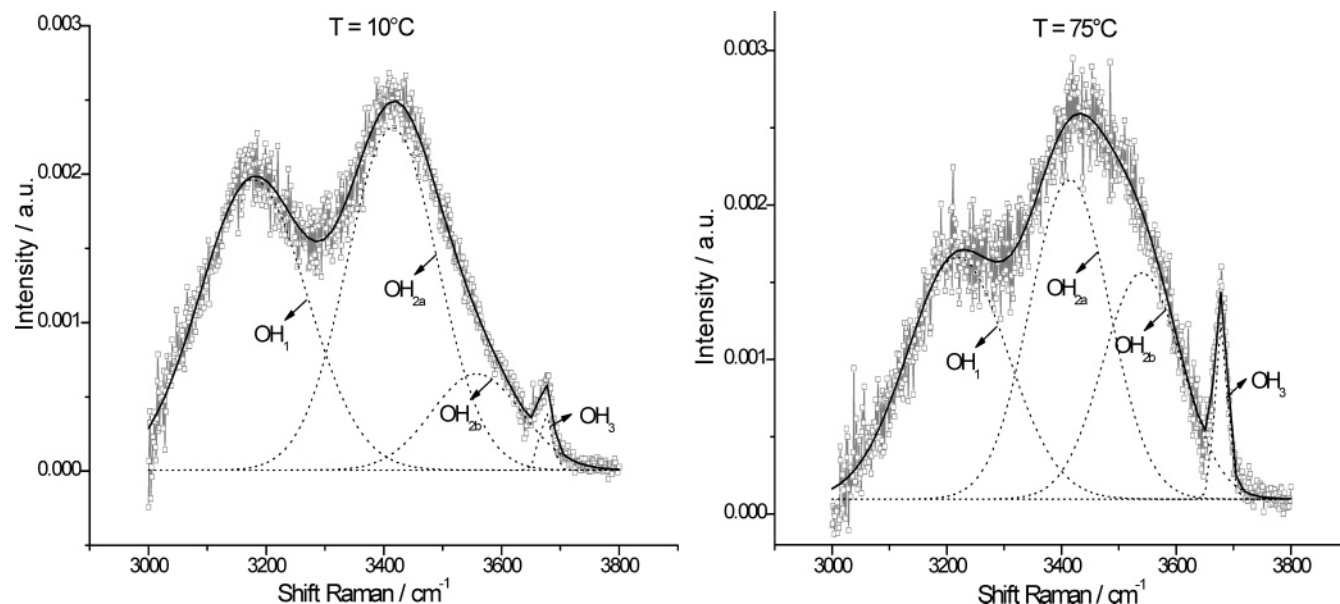


Figure 7. Water in octanol-rich solution: curve-fitting procedure applied to 10 and 75 °C VV subtraction spectra.

shows a significant increase. This happens also for the shoulder at higher frequencies around  $3650\text{ cm}^{-1}$  embodied in the OH-stretching envelope of the VV Raman spectrum of liquid water<sup>32</sup> (see Figure 6).

The position of OH<sub>2a</sub> and OH<sub>2b</sub> subbands is not clearly temperature dependent; on average, it seems that these frequencies remain quite constant. On the contrary, their intensities change significantly from 10 to 75 °C and tend to a redistribution that is in favor of the high-frequency constituent of the couple. In fact, assuming a single distribution of OH oscillators around the maximum of the OH<sub>2</sub> frequency, the increase of  $T$  would shift the band maximum toward the higher frequency OH<sub>2b</sub> component.

The results of the fitting procedure perfectly agree with the characteristics of intermolecular interactions probed by OH-stretching oscillator in bulk water. They confirm that the distribution of icelike oscillators (collective in phase OH<sub>1</sub> stretching band) progressively shifts toward higher frequencies on increasing temperature. This can be explained by assuming that the long-range structure characterized by tetrahedral aggregates reduces its spatial extension at the higher temperatures (blue shift of OH<sub>1</sub> component), but still persists at 75 °C.<sup>37</sup> On the contrary, the properties of the OH-stretching modes at higher frequencies do not change with respect to their position. This means that a Raman spectroscopic study in the region of OH stretching gives clear indications about the possibility of following the behavior of ordered and disordered H-bonded clusters even for a very low water content in solution. An increase of temperature will necessarily cause a reduction in the dimension of H-bonded aggregates, and this reduction will largely affect the properties of collective oscillators. In contrast, the OH-stretching bands associated with the disordered components will not suffer this different distribution of dimensions.

Walrafen<sup>42,43</sup> reproduced the room-temperature Raman OH-stretching contour of liquid water by means of four Gaussians centered at 3215(1), 3390(2), 3500(3), and 3620(4)  $\text{cm}^{-1}$ . These frequency values agree quite well with ours derived from the fitting analysis of subtraction spectra. It is widely recognized that the variation of temperature and/or pressure mainly influences the mode (1) contribution to the Raman contour.<sup>43</sup> Referring to these findings, our results of water in octanol are in perfect agreement with those of bulk water.

TABLE 3: HB and NHB Classes: Comparison between Pure Water and Water in Octanol

temp/°C	water in octanol $I_{\text{NHB}}/I_{\text{HB}}$	pure water $I_{\text{NHB}}/I_{\text{HB}}$
10	0.243	0.215
15	0.330	0.246
25	0.350	0.268
35	0.453	0.270
45	0.460	0.354
55	0.520	0.395
65	0.678	0.395
75	0.720	0.518

$$\Delta H_{\text{H}} = 3.01 \pm 0.25 \text{ kcal mol}^{-1} \quad \Delta H_{\text{H}} = 2.40 \pm 0.22 \text{ kcal mol}^{-1}$$

The Raman spectrum of liquid water has been often interpreted with a two-state model to give a quantitative estimation of two specific categories of OH bonds (not of water molecules). These two categories can be referred to as the couple “free-bonded”<sup>44</sup> or “non-H-bonded–H-bonded”<sup>32,33</sup> OH oscillators, divided with respect to the position of an isosbestic point (see Figure 6). The presence of the isosbestic point has been recognized in the temperature evolution of the OH-stretching profile both in VV and in HV configurations at 3403 and 3510  $\text{cm}^{-1}$ , respectively. Referring to the first of these two situations (VV profile), the integrated intensities of (1) and (2) components have been summed together to define the HB intensity ( $I_{\text{HB}}$ ), and those of (3) and (4) have been summed to define the NHB intensity ( $I_{\text{NHB}}$ ). Moreover, the  $I_{\text{NHB}}/I_{\text{HB}}$  values of water in SAT have been calculated considering corresponding components of subtraction spectra to define the two classes of oscillators.

The data of Table 3 show that the OH-stretching intensity distribution in the case of water in octanol enhances the high-frequency, NHB component with respect to pure water. The  $I_{\text{NHB}}/I_{\text{HB}}$  ratio can be reasonably assumed proportional to the equilibrium constant of  $\text{HB} \leftrightarrow \text{NHB}$ ;<sup>44</sup> as a consequence, a van’t Hoff treatment of these data can give an estimation of the enthalpy change  $\Delta H_{\text{H}}$  of the H-bond of pure water and of water in octanol. We find that the  $\Delta H_{\text{H}}$  value of pure water is  $2.40 \pm 0.22 \text{ kcal mol}^{-1}$ ; this datum is in good agreement with the literature value  $(\Delta H_{\text{H}})_{\text{L}}$  of  $2.54 \pm 0.10 \text{ kcal mol}^{-1}$  found with similar procedures.<sup>44–46</sup> The value that we find for water in octanol is still close to  $(\Delta H_{\text{H}})_{\text{L}}$  even if a bit higher:  $\Delta H_{\text{H}} = 3.01 \pm 0.30 \text{ kcal mol}^{-1}$ . Despite the approximations assumed in our procedures, the agreement between H-bonding variation



enthalphies above-mentioned is a further confirmation of the assignment of the subtraction spectrum to water confined in alcohol.

**3.5.2. Molecular Confinement.** In the past decade, examples of water confinement have been widely explored with a variety of different experimental techniques and computational methods,<sup>47–52</sup> and the argument is still of great interest in the scientific community.

In our opinion, the situation of water in octanol bears a close resemblance to the confinement of water between hydrophilic surfaces of micelles and large amphiphiles. In these cases, it has been asserted that the hydrogen bond structure of H<sub>2</sub>O is more disordered in comparison to the pure liquid.<sup>48,49</sup> Moreover, the analysis of the OH-stretching Raman profile shows that a distortion of the H-bonding network is more and more evident on diminishing the size of the polar cores, despite the chemical nature of the surface offered to water.<sup>49,50</sup> The spectroscopic properties of water confined on the mesoscopic scale are essentially connected to the intensity decrease of components associated to long-range-ordered water structures.<sup>48</sup> Self-associating properties of 1-octanol do not give a clear indication of inverse micelles formation; nevertheless, the distribution of alcohol clusters is such to create alternation of regions with polar and hydrophobic character. Values of octanol/water partition coefficients have been recently calculated by means of molecular dynamics (MD) simulations.<sup>51</sup> The results of this simulation are in perfect agreement with our spectroscopic findings because they show that there is a higher probability of finding a 1-octanol hydroxyl group H-bonded to other 1-octanol hydroxyl groups than to water molecules. Moreover, the situation proposed by De Oliveira et al.<sup>51</sup> suggests that water molecules would rather concentrate together in the proximity of 1-octanol OH groups.

From the point of view of our results, we can say that the self-association of water in octanol is reduced with respect to the pure liquid showing higher values of  $I_{\text{NHB}}/I_{\text{HB}}$  (see Table 3). Moreover, the analysis of OH-stretching Raman profiles show that, even if each subband of the spectrum of pure water is still present in SAT in the 10–75 °C range, each component of the total band is much sharper. This could suggest that the confinement in the water pockets gives typologies of OH oscillator very similar to those of the pure liquid but more definite regarding the distribution in different H-bonded aggregates.

According to the molecular dynamics simulation of MacCallum and Tieleman,<sup>13</sup> the arrangement of polar cores in SAT tends to form prolate ellipsoids rather than spheres. In this situation, the distribution of water molecules is probably limited to interactions with nearest or next-nearest neighbors. Even in this situation, the ordered, tetrahedrally coordinated water clusters ( $W_T$  clusters) are largely probable in the liquid system. A recent Monte Carlo simulation of pure liquid water shows that a molecular-level description for the formation of icelike regions implies the existence of  $W_T$  linear or ramified clusters rather than three-dimensional, clathratelike objects.<sup>52</sup> Within the results of this simulation, the local, microscopic scenario offered by liquid water shows the presence of both disordered and highly ordered linear aggregates. Moreover, these aggregates of tetrahedrally coordinated molecules are not much extended in size even at low temperatures.

We think that this latter simulation describing the molecular origin of the three-dimensional structure of pure H<sub>2</sub>O<sup>52</sup> perfectly fits with our results. In this sense, we suggest that, because of reduced (absent?) water–alcohol interactions, for water in SAT we find the same self-organizing tendencies present in the pure

liquid. Referring to the molecular origin of H-bonding aggregates, we propose the situation of water in octanol as an example of “molecular confinement”. The “molecular dimension” of the confinement means that the H<sub>2</sub>O pockets are very limited in extension (more limited than in micelles or nanopores), even showing an OH-stretching Raman profile very similar to that of bulk water. In particular, the similarities refer to the description of different types of OH oscillators; differences are envisaged in the distribution of H-bonded aggregates.

The confinement of water in the hydrophilic environments of liquid octanol, as observed through our spectroscopic results, can be referred to as the extension of water confinement in reverse micelles to the limit of very small pores dimensions.

## 4. Conclusions

The properties of liquid alcohols are connected to the amphiphilic nature of their molecules. The addition of water to *n*-alkanols realizes mixtures having anomalous thermodynamic and transport properties, due to the balance between hydrophobic and hydrophilic hydration effects.

Among the aqueous alcohols, octanol plays a very important role because of the large use as a membrane mimetic. Even if 1-octanol cannot self-organize to give micelles or layers,<sup>21</sup> the liquid structure of this system may resemble in some way the arrangement of large biomolecules in physiologic conditions.<sup>53</sup> In this perspective, the possibility of revealing the effects of water solubilization in octanol is particularly important because the mixture is even closer to the characteristics of biosystems.

In short-chain alcohols, steric factors and low hydrophobic character favor complete mixing with the presence of mixed clusters in the H-bonding networks. In our system where molecular dimensions are strongly different and the hydrophobic effects are large, one obtains a saturation limit and water is not able to perturb the alcohol aggregates; it rather self-arranges in a segregation state near the polar heads of octanol molecules.

In this respect, it is worth noting that in water solution of long poly(ethylene oxide), where the epoxy (O–CH<sub>2</sub>–CH<sub>2</sub>) repetition unit balances hydrophobic and hydrophilic effects within the chain, water introduces itself among the polymeric chain, creating stable and extended H-bonded networks.<sup>54</sup> In these cases, macroscopic quantities such as adiabatic compressibility and shear viscosity were found to largely depend on the increasing water content in solution. Differently, in our system, the compressibility is almost not sensitive to the presence of water.

The results of our Raman, depolarized-Rayleigh, and Brillouin measurements on water-saturated solution in the 10–70 °C temperature range give a clear indication of the maintained structural properties of the *n*-alcohol with respect to the pure state. Moreover, the temperature and polarization behavior of Raman OH-stretching profiles suggests that the properties of H<sub>2</sub>O in SAT are very close to those of bulk water, and then that a microheterogeneous environment for the distribution of components of the mixture is realized.

This microheterogeneous distribution of the two liquids is composition dependent in different alcohols. In alcohol-rich solutions, it may be connected to the hydrophilic hydration of the polar head and maintains similar properties in the different *n*-alkanols. On the contrary, on increasing the water content, the hydrophobic hydration largely depends on the characteristics of the alkylic chain.

Referring to the water confinement in 1-octanol polar regions, we propose a description in terms of “molecular confinement”



according to the reduced extension of H-bonded structures with respect to the cases of water in nanopores or micelles.

## References and Notes

- (1) Francks, F.; Ives, D. J. G. *Q. Rev.* **1966**, 20, 1.
- (2) Murrell, J. N.; Jenkins, A. D. *Properties of Liquids and Solutions*, 2nd ed.; Wiley: Chichester, 1994; p 102.
- (3) Nellist, P. D.; Pennicook, S. J. *Science* **1996**, 274, 413.
- (4) Fidler, J.; Rodger, P. M. *J. Phys. Chem. B* **1999**, 103, 7695.
- (5) Bowron, D. T.; Diaz-Moreno, S. *J. Chem. Phys.* **2002**, 117, 3753.
- (6) Dixit, S.; Poon, W. C. K.; Crain, J. J. *Phys.: Condens. Matter* **2000**, 12, L323.
- (7) Dixit, S.; Crain, J.; Poon, W. C. K.; Finney, J. L.; Soper, A. K. *Nature* **2002**, 416, 829.
- (8) Sato, T.; Buchner, R. *J. Chem. Phys.* **2003**, 119, 10789.
- (9) Kusalik, P. G.; Lyubartsev, A. P.; Bergman, D. L.; Laaksonen, A. *J. Phys. Chem. B* **2000**, 104, 9526.
- (10) Bowron, D. T.; Diaz-Moreno, S. *J. Phys.: Condens. Matter* **2003**, 15, S121.
- (11) Onori, G.; Santucci, A. *J. Mol. Liq.* **1996**, 69, 161.
- (12) Freda, M.; Onori, G.; Cantucci, A. *Phys. Chem. Chem. Phys.* **2002**, 4, 4979.
- (13) MacCallum, J. L.; Tieleman, D. P. *J. Am. Chem. Soc.* **2002**, 124, 15085.
- (14) Paolantoni, M.; Sassi, P.; Morresi, A.; Cataliotti, R. S. *Mol. Phys.* **2001**, 99, 1493.
- (15) Sassi, P.; Morresi, A.; Paolantoni, M.; Cataliotti, R. S. *J. Mol. Liq.* **2002**, 96–97, 361.
- (16) Sassi, P.; Paolantoni, M.; Morresi, A. *Chem. Phys. Lett.* **2002**, 357, 293.
- (17) Sassi, P.; Marcelli, A.; Paolantoni, M.; Morresi, A.; Cataliotti, R. S. *J. Phys. Chem. A* **2003**, 107, 6243.
- (18) Raudino, A.; Sassi, P.; Morresi, A.; Cataliotti, R. S. *J. Chem. Phys.* **2002**, 117, 4907.
- (19) Berti, P.; Cabani, S.; Mollica, V. *Fluid Phase Equilib.* **1987**, 32, 195.
- (20) von Erichsen, L. *Brennst. Chem.* **1952**, 33, 166.
- (21) DeBolt, S. E.; Kollman, P. A. *J. Am. Chem. Soc.* **1995**, 117, 5316.
- (22) Sato, T.; Chiba, A.; Nozaki, R. *J. Chem. Phys.* **2000**, 112, 2924.
- (23) Sato, T.; Chiba, A.; Nozaki, R. *J. Mol. Liq.* **2002**, 101, 99.
- (24) Paolantoni, M.; Ladanyi, B. M. *J. Chem. Phys.* **2002**, 117, 3856.
- (25) Gestblom, B.; Sjöblom, J. *Acta Chem Scand.* **1984**, 38, 47.
- (26) Shinomiya, T. *Bull. Chem. Soc. Jpn.* **1989**, 62, 908.
- (27) Petong, P.; Pottel, R.; Kaatz, U. *J. Phys. Chem. A* **2000**, 104, 7420.
- (28) Behrends, R.; Kaatz, U. *J. Phys. Chem. A* **2001**, 105, 5829.
- (29) Kaatz, U.; Behrends, R.; Pottel, R. *J. Non-Cryst. Solids* **2002**, 305, 19.
- (30) Ratcliffe, C. I.; Irish, D. H. *J. Phys. Chem.* **1982**, 86, 4897.
- (31) Danten, Y.; Tassaing, T.; Besnard, M. *J. Phys. Chem. A* **2000**, 104, 9415.
- (32) Walrafen, G. E.; Hokmabadi, M. S.; Yang, W.-H. *J. Chem. Phys.* **1986**, 85, 6964.
- (33) Walrafen, G. E.; Fisher, M. R.; Hokmabadi, M. S.; Yang, W.-H. *J. Chem. Phys.* **1986**, 85, 6970.
- (34) Graener, H.; Ye, T. Q.; Laubereau, A. *J. Chem. Phys.* **1989**, 90, 3413; **1989**, 91, 1043.
- (35) Levinger, N. E.; Davis, P. H.; Fayer, M. D. *J. Chem. Phys.* **2001**, 115, 9352.
- (36) Gaffney, K. J.; Davis, P. H.; Piletic, I. R.; Levinger, N. E.; Fayer, M. D. *J. Phys. Chem. A* **2002**, 106, 12012.
- (37) Green, J. L.; Lacey, A. R.; Sceats, M. G. *J. Phys. Chem.* **1986**, 90, 3958.
- (38) Hansch, C.; Leo, A. J. *Substituent Constants for Correlation Analysis in Chemistry and Biology*; Wiley: New York, 1979.
- (39) Hansch, C.; Bjorkroth, J. P.; Leo, A. J. *J. Pharm. Sci.* **1987**, 76, 663.
- (40) Martinez, M. N.; Amidon, G. L. *J. Clin. Pharmacol.* **2002**, 42, 620.
- (41) Jensen, M. Ø.; Mouritsen, O. G.; Peters, G. H. *J. Chem. Phys.* **2004**, 120, 9729.
- (42) Walrafen, G. E. In *Structure of Water and Aqueous Solutions*; Luck, W. A. P., Ed.; Verlag Chemie, Physik Verlag: Weinheim, 1974.
- (43) Walrafen, G. E.; Chu, Y. C. *J. Phys. Chem.* **1995**, 99, 11225.
- (44) Carey, D. M.; Korenowski, G. M. *J. Chem. Phys.* **1998**, 108, 2669.
- (45) Walrafen, G. E. In *Water: a comprehensive treatise*; Franks, F., Ed.; Plenum: New York, 1971; Vol. 1.
- (46) Bansil, R.; Wiafe-Akenten, J.; Taaffe, J. L. *J. Chem. Phys.* **1982**, 76, 2221.
- (47) Levinger, N. E. *Nature* **2002**, 298, 1722.
- (48) Marinov, V. S.; Nickolov, Z. S.; Matsuura, H. *J. Phys. Chem. B* **2001**, 105, 9953.
- (49) Crupi, V.; Magazù, S.; Maiolino, D.; Maisano, G.; Migliardo, P. *J. Mol. Liq.* **1997**, 80, 13S.
- (50) Lafleur, M.; Pigeon, M.; Pézolet, M.; Caillé, J. P. *J. Phys. Chem.* **1989**, 93, 1522.
- (51) De Oliveira, C. A. F.; Guimaraes, C. R. W.; De Alencastro, R. B. *Int. J. Quantum Chem.* **2002**, 90, 786.
- (52) Errington, J. R.; Debenedetti, P.; Torquato, S. *Phys. Rev. Lett.* **2002**, 89, 215503.
- (53) Wimley, W. C.; Creamer, T. P.; White, S. H. *Biochemistry* **1996**, 35, 5109.
- (54) Magazù, S.; Maisano, G. *J. Mol. Liq.* **2001**, 93, 7.